

Original Article

Axl inhibitor R428 induces apoptosis of cancer cells by blocking lysosomal acidification and recycling independent of Axl inhibition

Fangfang Chen^{1,2}, Qiaoling Song^{1,2}, Qiang Yu^{1,2}

¹Shanghai Institute of Materia Medica, Chinese Academy of Sciences, Shanghai 201203, China; ²University of Chinese Academy of Sciences, Beijing 100049, China

Received June 5, 2018; Accepted July 9, 2018; Epub August 1, 2018; Published August 15, 2018

Abstract: R428 (BGB324) is an anti-cancer drug candidate under clinical investigation. It inhibits the receptor tyrosine kinase Axl and induces apoptosis of many types of cancer cells, but the relationship between the two has not been well established. We investigated the molecular mechanisms of the R428-induced apoptosis and found that R428 induced extensive cytoplasmic vacuolization and caspase activation, independent of its inhibitory effects on Axl. Further analyses revealed that R428 blocked lysosomal acidification and recycling, accumulated autophagosomes and lysosomes, and induced cell apoptosis. Inhibition of autophagy by autophagy inhibitors or autophagic gene-knockout alleviated the R428-induced vacuoles formation and cell apoptosis. Our study uncovered a novel function and mechanism of R428 in addition to its ability to inhibit Axl. These data will help to better direct the application of R428 as an anti-cancer reagent. It also adds new knowledge to understand the regulation of autophagy and apoptosis.

Keywords: R428, Axl, cancer cells, apoptosis, autophagy, vacuolization

Introduction

Axl is one of the three members of the TAM (Tyro3, Axl, and Mer) receptor tyrosine kinase family and plays critical roles in regulating cell survival, proliferation, adhesion, and migration [1-3]. Overexpression or activation of Axl has been linked to high invasiveness and metastasis of many types of cancers [2]. It has also been found to be a key player in the acquired resistance of cancer cells to targeted therapies [4]. For example, upregulation of Axl in cancer cells has been found to be the second most prevalent mechanism of resistance to EGFR inhibitors in addition to the T90M mutation of EGFR [5].

Because of its critical roles in cancer formation and progression, Axl has been considered as a promising target for cancer drug development. Small molecule inhibitors of Axl therefore have attracted increasing attentions. R428 (BGB-324) is one of the highly potent and frequently studied Axl inhibitors, which blocks Axl auto-

phosphorylation on its C-terminal docking site, Tyr821, at nanomolar concentrations [2, 3]. R428 is also the first Axl inhibitor to enter clinical trials in 2014 due to its superiority in inhibiting metastases of cancer cells in vitro and in animal models. It is now in Phase I/II clinical trials of TNBC, metastatic melanoma, and NSCLC in combination with pembrolizumab, Dabrafenib/Trametinib, or erlotinib (ClinicalTrials.gov Identifier: NCT03184571, NCT03184558, NCT02872259 and NCT02424617). The molecular mechanisms of R428 in regulating cancer cell growth and metastasis however have not been thoroughly investigated. It has been reported that R428 induced cancer cell apoptosis [6, 7], but the role of Axl inhibition in the R428-induced apoptosis has not been clear.

Autophagy is a catabolic process sensitive to metabolic stress and is activated to remove unnecessary or dysfunctional cellular components, including organelles and proteins, mediated by lysosomal hydrolases and subsequently recycled to sustain cellular metabolism [8, 9].

R428 induces cancer cell apoptosis by blocking lysosomal acidification

Autophagy consists of a series of events, starting with an inclusion of unwanted cytoplasm into an elongating phagophore to form a double-membrane autophagosome, followed by fusion with lysosomes to generate autolysosomes, in which protein digestion occurs. At the end, lysosomal membrane components are extruded from autolysosomes to become “pro-lysosomes”, which eventually reform into functional lysosomes by maturation (autophagic lysosome reformation, ALR) [10-12]. In the course of autophagy, lysosomal function is activated after autophagosome-lysosome fusion to maintain a highly acidic lumen (pH 4.5-5.0) for proteolysis [12]. The series events of autophagy are highly regulated and dysregulation of autophagy have been linked to cell apoptosis. However, the roles of autophagy in apoptosis regulation are complex. On one hand, autophagy blocks induction of apoptosis by removing damaged mitochondria, pro-apoptotic proteins, and ROS in certain vulnerable cells. On the other hand, autophagy or autophagy-related proteins may facilitate apoptosis by activating caspases or depleting endogenous apoptotic inhibitors [13, 14]. The precise relationship between autophagy and apoptosis is still an active area of research.

In the present study, we investigated the molecular mechanisms of R428 in inhibiting cancer cell growth and found that R428 caused dilation of lysosomes, blocked autophagic degradation, and induced cell apoptosis, all of which were independent of Axl inhibition. Our study provided new information on understanding the activities of R428 and the relationship between autophagy and apoptosis, which will help to better use R428 as an anti-cancer agent.

Materials and methods

Cell line

Bel7404, SMMC7721, H4-LAMP1-GFP [15], H4-GFP-LC3 [16], MEFs and MEFs (Atg5^{-/-}) [17] were gifts from Prof. Junying Yuan (Interdisciplinary Research Center on Biology and Chemistry, Shanghai Institute of Organic Chemistry, Shanghai, China). LM3 was a gift from Prof. Hongyang Wang (Eastern Hepatobiliary Surgery Institute, Shanghai, China). All other cell lines were obtained from the American

Type Culture Collection. The H1299, Bel7404, H1650, 97H, Bel7402, MB231 and A549 cells were cultured in RPMI1640 medium (Invitrogen) with 10% FBS. The HeLa, LM3, H4-LAMP1-GFP, H4-GFP-LC3, MB453, PC9, H4, MEFs and MEFs (Atg5^{-/-}) cells were cultured in DMEM medium (Invitrogen) with 10% FBS. The SW1116 cells were cultured in MEM medium (Invitrogen) with 10% FBS.

Reagents

The sources of chemicals, antibodies and dyes were as follows:

R428 (# A8329, APEX BIO), LDC1267 (# S7638, Selleck), Z-VAD-FMK (# S7023, Selleck), SB-203580 (# S1076, Selleck), chloroquine (CQ) (# c6628, Sigma-Aldrich). Spautin-1 (C43), pyriminidinium pamoate (PP) and bafilomycin (Baf A1) were gifts from Prof. Junying Yuan (Shanghai Institute of Organic Chemistry, Shanghai, China).

α -Tubulin (# SC-5286, Santa Cruz Biotechnology), PARP (# 556494, BD Pharmingen Technical), β -actin (# P30002M, Abmart). The following antibodies were purchased from Cell Signaling Technology: phospho-Axl (# 5724), Axl (# 4566), cleaved PARP (# 9541), caspase-8 (# 9746), caspase-9 (# 9502), Bcl-2 (# 2876), Bcl-xl (# 2762), LC3B (# 3868), SQSTM1/p62 (# 8025), phospho-EGFR (# 3777), EGFR (# 4267). Recombinant Human Gas6 Protein (# 885-GSB, R&D).

Neutral Red (NR) (# 71028260, Sinopharm Chemical Reagent Co., Ltd.), acridine orange (Biosharp), Propidium iodide (PI) (# P4170, Sigma-Aldrich), Lyso-tracker Red (# C1046, Beyotime).

Western blotting

Western blotting was performed as previously described [18]. Immune complexes were incubated with Immobilon Western Chemiluminescent HRP Substrate (Millipore) for 2-3 min, and then photographed using Darkroom Eliminator (C300, AZURE biosystems).

Cell staining and microscopy

PI staining: Cells were plated in 1 ml medium at 1×10^5 cells/well in 12-well plates one day before use. After drug treatment, PI (1 mg/ml in

R428 induces cancer cell apoptosis by blocking lysosomal acidification

DMSO) was added to the culture medium to a final concentration of 1 µg/ml and real time images were captured at 2-hours intervals with Leica Microsystems CMS GmbH, Ernst-Leitz-Str. 17-37 (11525103) with rhodamine filter settings.

NR or AO staining: Cells were plated in 500 µl medium at 5×10^4 cells/well in 24-well plates one day before use. After drug treatment, NR (28 mg/ml in DMSO) was added to culture medium to a final concentration of 28 µg/ml for 15 minutes and washed out with PBS. Phase-contrast images were captured with Leica DMI3000 B in 10 minutes. For AO staining, AO (5 mg/ml in H₂O) was added to culture medium to a final concentration of 5 µg/ml for 15 minutes and then replaced with fresh medium for imaging. Fluorescent images were captured with Leica DMI3000 B with GFP filter settings [19].

Immunofluorescence analysis: Immunofluorescence analysis was performed as previously described [20]. For lyso-tracker red staining, lyso-tracker red was added to culture medium to a final concentration of 50 nM for 30 minutes at 37°C and then washed out with cold PBS. After fixation with 4% paraformaldehyde for 20 minutes at room temperature, the cell nucleus was stained with 15 min-incubation of 2 µg/ml Hoechst.

RNAi and transfection

Axl siRNA (sc-29769) was purchased from SANTA CRUZ biotechnology. SiRNAs were transfected into cells using Lipofectamine 2000 or 3000 (Invitrogen).

Transmission electron microscopy

Bel7404 cells were plated in 10 cm-dishes overnight and incubated with DMSO or R428 for 24 hours. Cell samples were fixed with fixing solution provided by Prof. Jing Yi laboratory (School of Medicine, Shanghai Jiaotong University, Shanghai, China) and collected by scraping. All samples were sent to Prof. Jing Yi laboratory for transmission electron imaging.

Real-time quantitative PCR assay

Cell lysates were collected after trizol incubation and total RNA was extracted for further

experiments. The mRNA abundances of autophagy-related genes were quantified by real-time qPCR assay. The Real-time Quantitative PCR Assay was performed as previously described [21], and GAPDH was used as an endogenous control. The sequences of primers are as follows: human MAP1LC3, forward: 5'-AACATG-AGCGAGTTGGTCAAG-3', reverse: 5'-GCTCGTAGTGTCGCGAT-3'; human SQSTM1/p62, forward: 5'-GCACCCAATGTGATCTGC-3', reverse, 5'-CGCTACACAAGTCGTAGTCTGG-3'; human GAPDH, forward, 5'-ACCACAGTCCATGCCATCAC-3', reverse, 5'-TCCACCACCCTGTTGCTG-3' [22]; human Gas6, forward, 5'-TCTTCTACACTGTGCTG-TTGCG-3', reverse, 5'-GGTCAGGCAAGTTCTGAA-CACAT-3' [23].

Statistical analyses

Data were graphically represented as mean ± SD. Statistical analyses were performed by Prism version 6.0 (GraphPad Prism Software). All experiments were replicated at least 3 times.

Results

R428 induced apoptosis of cancer cells independent of Axl inhibition

To understand the role of Axl inhibition in the R428-induced cell death, we compared the effects of R428 on cancer cell growth with that of a different Axl inhibitor LDC1267 [24]. R428 inhibited growth of H1299, a human non-small cell lung carcinoma cell line that had constitutively activated Axl, in a dose-dependent manner with an IC₅₀ of approximately 4 µM, while LDC1267 had no effects on the cell growth even at 20 µM (**Figure 1A**). However, the effects of the two compounds on the tyrosine phosphorylation of Axl was opposite of that on cell growth. In R428 treatment, Axl phosphorylation was inhibited but bounced back in 6 hours, without inducing its ligand, Gas6 expression (**Figures 1B** and **S1A**). Contrarily, LDC1267 was a much more persistent inhibitor of Axl phosphorylation (**Figure 1B**). Furthermore, R428 induced PARP cleavage while LDC1267 did not (**Figure 1B**).

The cell death inducing activity of R428 was further investigated in a different cancer cell line, the cervical cancer cell line Hela, that had

R428 induces cancer cell apoptosis by blocking lysosomal acidification

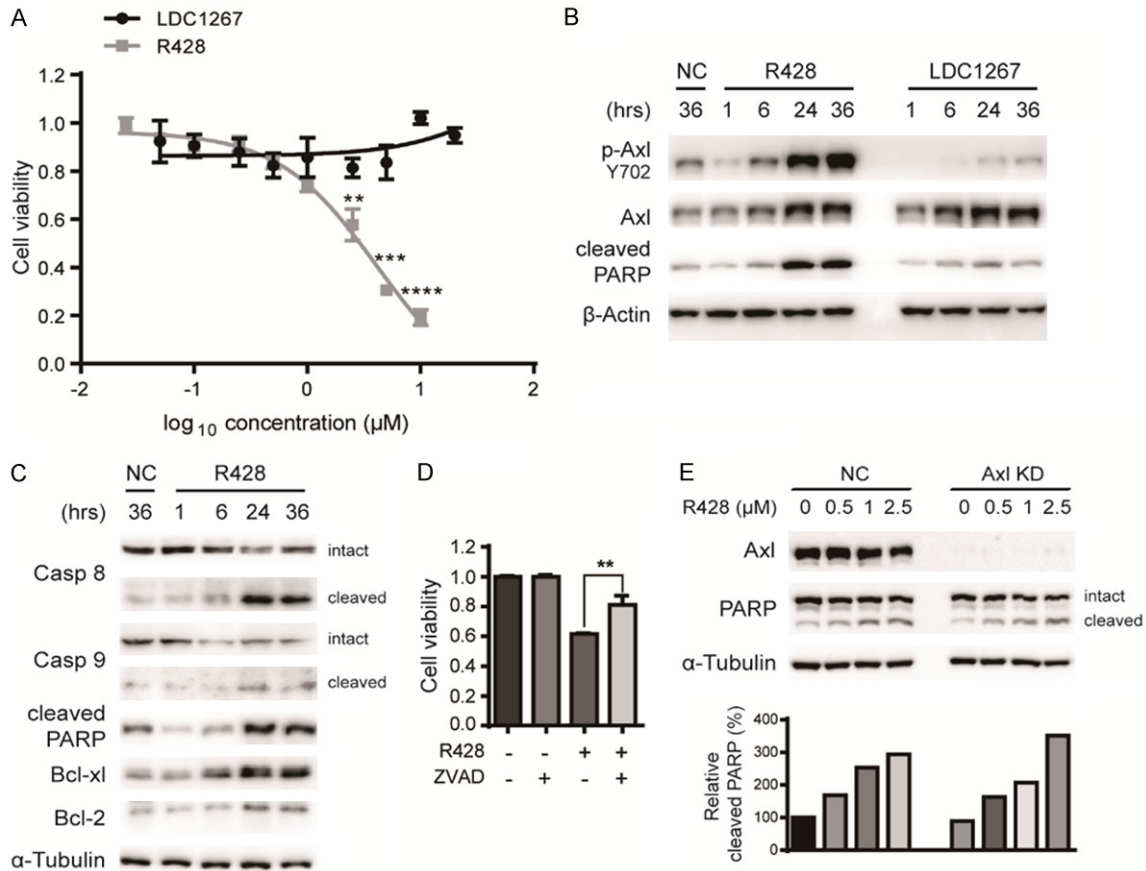


Figure 1. The cell growth-inhibition and apoptosis induced by R428 were Axl-independent. **A.** H1299 cells were cultured with the indicated concentrations of R428 or LDC1267 for 48 hours. Cell viability was evaluated by MTT assay. **, $P < 0.01$; ***, $P < 0.001$; ****, $P < 0.0001$, Student's T test. Error bars, mean \pm SD. **B.** H1299 cells were treated with DMSO (NC, negative control), 2.5 μ M R428, or 0.5 μ M LDC1267 for indicated time periods. Total cell lysates were processed for western blotting analysis using antibodies as indicated. **C.** HeLa cells were treated with DMSO (NC, negative control) or 2.5 μ M R428 for indicated time periods. Total cell lysates were processed for western blotting analysis using antibodies as indicated. Casp 8, caspase-8. Casp 9, caspase-9. **D.** HeLa cells were treated with DMSO or 2.5 μ M R428 in the presence or absence of 10 μ M Z-VAD-FMK (ZVAD) for 72 hours. Cell viability was evaluated by MTT assay. **, $P < 0.01$, Student's T test. Error bars, mean \pm SD. **E.** HeLa cells were pretreated without or with Axl silencing RNA (NC or Axl KD) for 24 hours, and then cultured with indicated concentrations of R428 for another 36 hours. Total cell lysates were processed for western blotting analysis using antibodies as indicated. The histogram below indicates the quantitation of the cleaved PARP on the western blot relative to the control normalized by α -Tubulin.

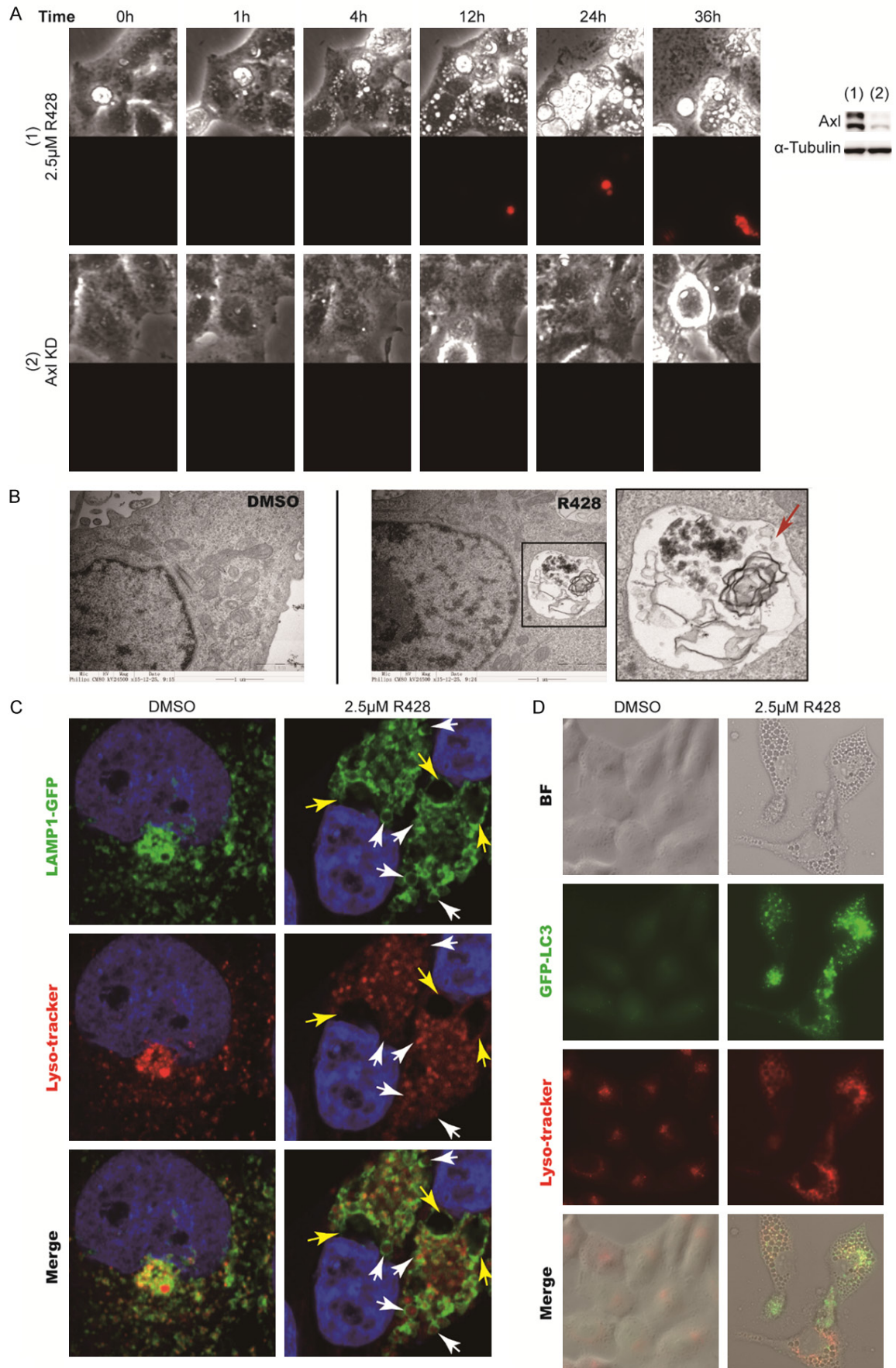
normal Axl phosphorylation. R428 induced a series of apoptotic events, including caspase-8/9 activation, PARP cleavage, and up-regulation of anti-apoptotic proteins Bcl-xl and Bcl-2 in the HeLa cells (Figure 1C). Z-VAD-FMK, a pan-caspase and apoptosis inhibitor [25], alleviated the R428-induced cell death (Figure 1D). These data suggested that there was no correlation between the inhibition of Axl phosphorylation and apoptosis induction of R428.

To exclude the involvement of Axl in the R428-induced apoptosis, we knocked down the Axl

gene expression by siRNA and analyzed the effects of R428 on the Axl-knock-down cells. R428 induced PARP cleavage and cell death similarly with or without the expression of Axl (Figure 1E).

Taken together, these results suggested that R428 induced cancer cell apoptosis not through inhibiting Axl. There must be additional targets that were responsible for the R428-induced apoptosis. The data also suggested that inhibition of Axl might not be sufficient to block cancer cell growth.

R428 induces cancer cell apoptosis by blocking lysosomal acidification



R428 induces cancer cell apoptosis by blocking lysosomal acidification

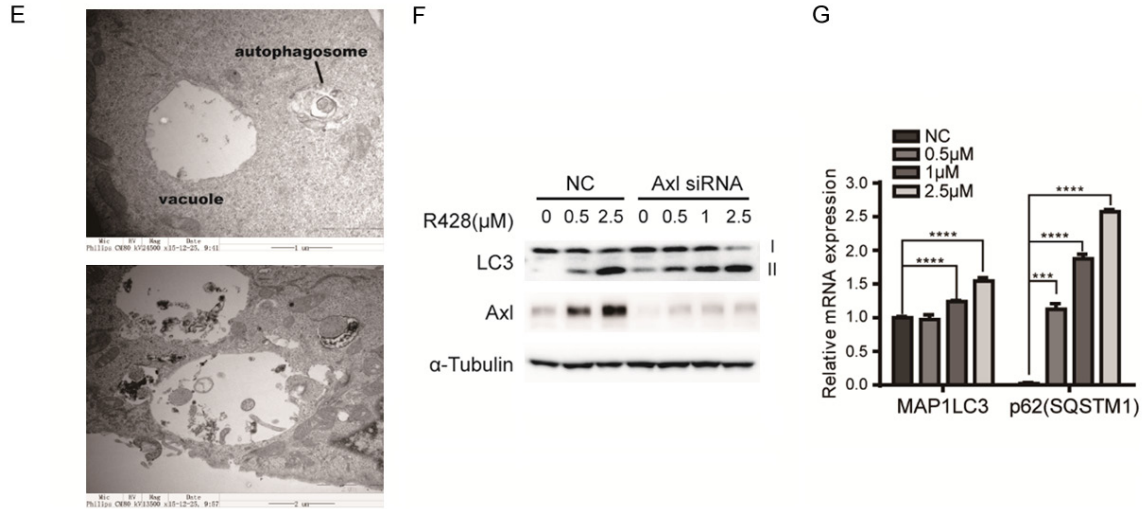


Figure 2. R428 induced lysosomal vacuolization and increased lysosomes and autophagosomes independent of Axl inhibition. A. LM3 cells were transfected with or without Axl silencing RNA (Axl KD) for 24 hours, and then were cultured with or without 2.5 μ M R428 for additional time periods as indicated (0-36 hr). Cells were stained with 1 μ g/ml Propidium iodide (PI) and the dead cells were stained red. Magnification: $\times 200$. The western blot on the right illustrated the siRNA knock-down result. B. Bel7404 cells were treated with DMSO or 0.5 μ M R428 for 24 hours, and the vacuoles were examined by TEM analysis. The picture on the right is an enlargement of the section in a black frame. Dark condensation marked by a red arrow was suspected to be the product undergoing degradation. C. H4-LAMP1-GFP cells were treated with DMSO or 2.5 μ M R428 for 24 hr and stained with 50 nM lysosome-tracker red. 2 μ g/ml Hoechst was used to stain nucleus. Fixed samples were visualized by confocal microscopy. Magnification: $\times 600$. Yellow arrows indicate the undyed vacuoles. D. H4-GFP-LC3 cells were treated with DMSO or 2.5 μ M R428 for 24 hr, and then stained with 50 nM lysosome-tracker red for another 30 min. GFP-LC3 puncta and lysosomes were visualized by a fluorescence microscope. Magnification: $\times 400$. BF, bright field. E. Representative TEM images of 0.5 μ M R428-treated Bel7404 cells. The image on the top showed a cytoplasmic vacuole and an autophagosome. The image below showed an autophagosome fusing with a vacuole. The scale bars in these diagrams represent 1 μ m. F. H4-GFP-LC3 cells were pretreated without or with Axl siRNA (NC or Axl siRNA) for 24 hours, and were then cultured with indicated concentrations of R428 for additional 24 hours. Total cell lysates were processed for western blotting using antibodies as indicated. G. RT-qPCR analysis of LC3 (MAP1LC3) and p62 (SQSTM1) mRNA expression in H4-GFP-LC3 cells which were treated with or without indicated concentrations of R428 for 24 hr. ***, $P < 0.001$ and **** $P \leq 0.001$, Student's T test. Error bars, mean \pm SD.

R428 induced vacuoles formation and autophagy

To understand the molecular mechanisms of the R428-induced apoptosis, we first examined the morphological changes of the dying cells. We observed that R428 induced cytoplasmic vacuoles within one hour after R428 treatment, and the vacuoles increased in number and size with time (**Figure 2A**). Part of the cells stained positive with Propidium iodide at later stages of the treatment, indicating dead cells (**Figure 2A**). However, knocking down Axl with siRNA did not cause vacuolization and cell death (**Figure 2A**), again suggesting that R428 induced vacuolization and cell death not through inhibiting Axl.

To understand the nature of the vacuoles, we examined the ultrastructure of the vacuoles by

transmission electron microscope (TEM) and found that these vacuoles were bounded by a single membrane and contained dense materials inside, similar to those in lysosomes [26], suggesting that the vacuoles might be derived from lysosomes (**Figure 2B**).

To confirm the lysosomal origin of these vacuoles, a human glioblastoma cell line H4-LAMP1-GFP, which expresses the LAMP1-GFP fusion protein (lysosomal associated protein-GFP fusion protein), was used to monitor the changes of lysosomes during R428 treatment [15]. After 24 hr R428 treatment, the LAMP1-GFP-labeled lysosomes dilated into large vacuoles, demonstrating that these vacuoles were derived from lysosomes (**Figure 2C**). In addition, most of the LAMP1-GFP-labeled vacuoles were also stained positive with the lysosome-tracker, a fluorescent lysosomal marker which stains the acidic

R428 induces cancer cell apoptosis by blocking lysosomal acidification

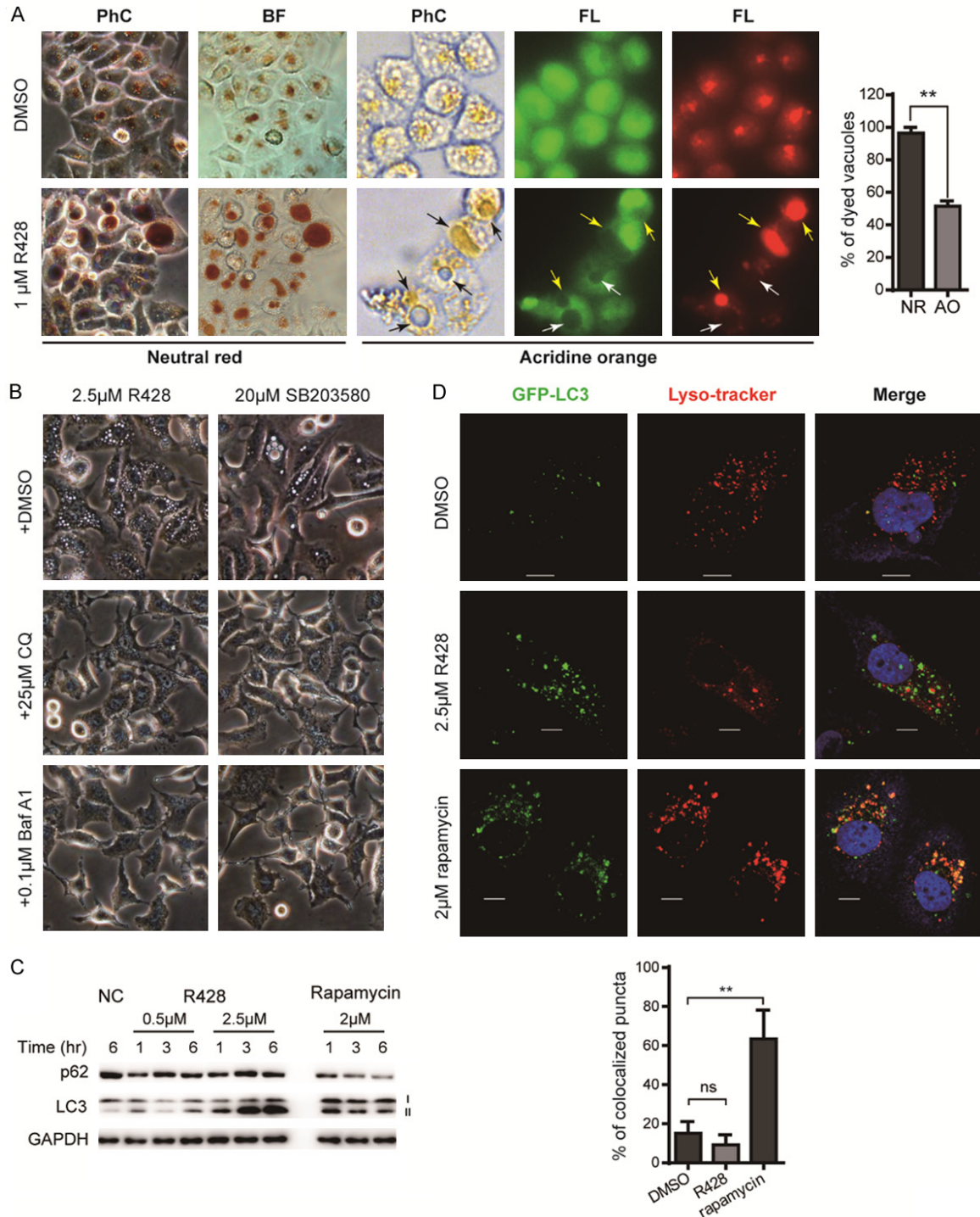


Figure 3. R428 altered the lysosomal pH and blocked autophagic degradation. **A.** Bel7404 cells were treated with DMSO or 1 μ M R428 for 48 hr and then stained with neutral red (NR) or acridine orange (AO). NR accumulated in acidic vacuoles within 10 min (left panel). AO stained the cytoplasm and nucleus green and the acidic vacuoles orange-red [27, 46]. The arrows point to the vacuoles. Percentage of the stained to the total vacuoles was calculated by ImageJ and plotted on the right of the picture. $**P \leq 0.005$, Student's T test. Error bars, mean \pm SD. PhC, phase-contrast. BF, bright field. FL, fluorescent light. Magnification: $\times 100$ (NR) or $\times 200$ (AO). **B.** A549 cells were treated with chloroquine (CQ) or bafilomycin A1 (Baf A1) with R428 or SB203580 for 24 hr. Phase-contrast images were taken at the magnification of 200 \times . **C.** H4-GFP-LC3 cells were lysed after culturing with R428 or rapamycin for indicated time periods, and the protein levels of LC3, p62 were detected by western blotting using antibodies as indicated. Anti-GAPDH antibody was used as a control. **D.** H4-GFP-LC3 cells were treated with DMSO, R428 (2.5

R428 induces cancer cell apoptosis by blocking lysosomal acidification

μM), or rapamycin ($2 \mu\text{M}$) for 24 hr, then stained with 50 nM lysosome-tracker red for another 30 min. Fixed samples were analyzed by confocal microscopy. $2 \mu\text{g/ml}$ Hoechst was used to stain nucleus. Percentage of the colocalized puncta to the total GFP-LC3 puncta was calculated from 3 independent samples by ImageJ and plotted below the picture. $**P \leq 0.005$. ns, no significance. Student's T test. Error bars, mean \pm SD. Bar, $10 \mu\text{m}$.

lysosomes and late endosomes [27]. The larger vacuoles, however, were lysosome-tracker-negative (**Figures 2C** and **S2A**), suggesting that the larger vacuoles might have different internal pH than that of the small ones and the normal lysosomes/late endosomes.

The number of the lyso-tracker-positive signals, indicating lysosomes and/or late endosomes, was also increased in the R428-treated cells (**Figures 2D** and **S2B**). In addition, we observed increased number of small double membrane-bounded vacuoles, resembling autophagosomes, in the R428-treated cells under TEM (**Figure 2E**), suggesting that R428 also induced autophagy.

To determine whether R428 affected autophagy, we treated a GFP-LC3-expressing human glioblastoma cell line H4-GFP-LC3 with R428 [16]. R428 significantly increased the number of autophagosomes as indicated by the aggregation of the GFP-LC3 (**Figures 2D** and **S2B**), which specifically localized to the membrane of autophagosomes [16, 28]. This result was further confirmed by western blotting analyses. R428 increased LC3-II level in a dose and time-dependent manner (**Figures 2F** and **3C**). Furthermore, the expressions of two autophagy-related genes, MAP1LC3 and p62/SQSTM1, were also increased by R428 treatment (**Figure 2G**). As a control, rapamycin, a known autophagic inducer [29, 30], only increased the number of autophagosomes and lysosomes, but not the large vacuoles (**Figure S2B**).

Like the R428-induced cell death and vacuoles formation, the autophagosome accumulation caused by R428 was again independent of Axl, because knocking down Axl by siRNA had no effects on the LC3-II induction by R428 (**Figure 2F**).

Taken together, these data suggested that lysosomes might be another target of R428. R428 might disturb the lysosome function and induce autophagy, leading to accumulation and fusion of autophagosomes and lysosomes to form the vacuoles, all of which were independent of Axl.

R428 altered the pH of lysosomes and blocked autophagic degradation

Above data suggested that the R428-induced vacuoles were derived from lysosomes or late endosomes. However, the failure of the larger vacuoles to be stained by the lyso-tracker red suggested that the pH inside of the larger vacuoles might not be as acidic as that of the lysosomes (**Figures 2C** and **S2A**), because the lyso-tracker red usually accumulates in low-pH organelles (pH 5) [31]. We then stained the R428-treated cells with two dyes of acidic organelles, the neutral red (NR) or the acridine orange (AO), both of which become protonated and appeared red in acidic environments, but the pH requirements are different. NR becomes red in weak pH while AO becomes red only in strong acidic (lower pH) organelles [27]. As shown in **Figure 3A**, NR became red in almost all the vacuoles while AO became red only in about 50% of them (**Figure 3A**), suggesting that the vacuoles were acidic but varied in their internal pH. Some of the protonated AO-negative vacuoles might have altered their internal pH that could no longer trapped enough protonated AO molecules but still were acidic enough to keep NR protonated. However, the low pH of lysosomes appeared necessary for R428 to induce vacuolization since concomitant treatment of the cells with R428 and bafilomycin (Baf A1) or chloroquine (CQ), two lysosomal lumen alkalizers [32, 33], alleviated the vacuolization induced by R428, which is consistent with SB203580, a molecule previously reported to induce acidic vacuoles formation (**Figure 3B**) [19]. These data suggested that R428 interacted with lysosomes, altered their internal pH, and enlarged them.

It's well-known that the highly acidic condition (pH 4.5-5.0) is strictly maintained by lysosome to execute protein degradation through internal hydrolases [12]. To investigate whether the altered pH of lysosomes by R428 inhibited autophagic degradation, we analyzed the level changes of LC3-II, an indicator of autophagy initiation, and p62, a chaperone known to be degraded in autolysosomes at the later stages of

R428 induces cancer cell apoptosis by blocking lysosomal acidification

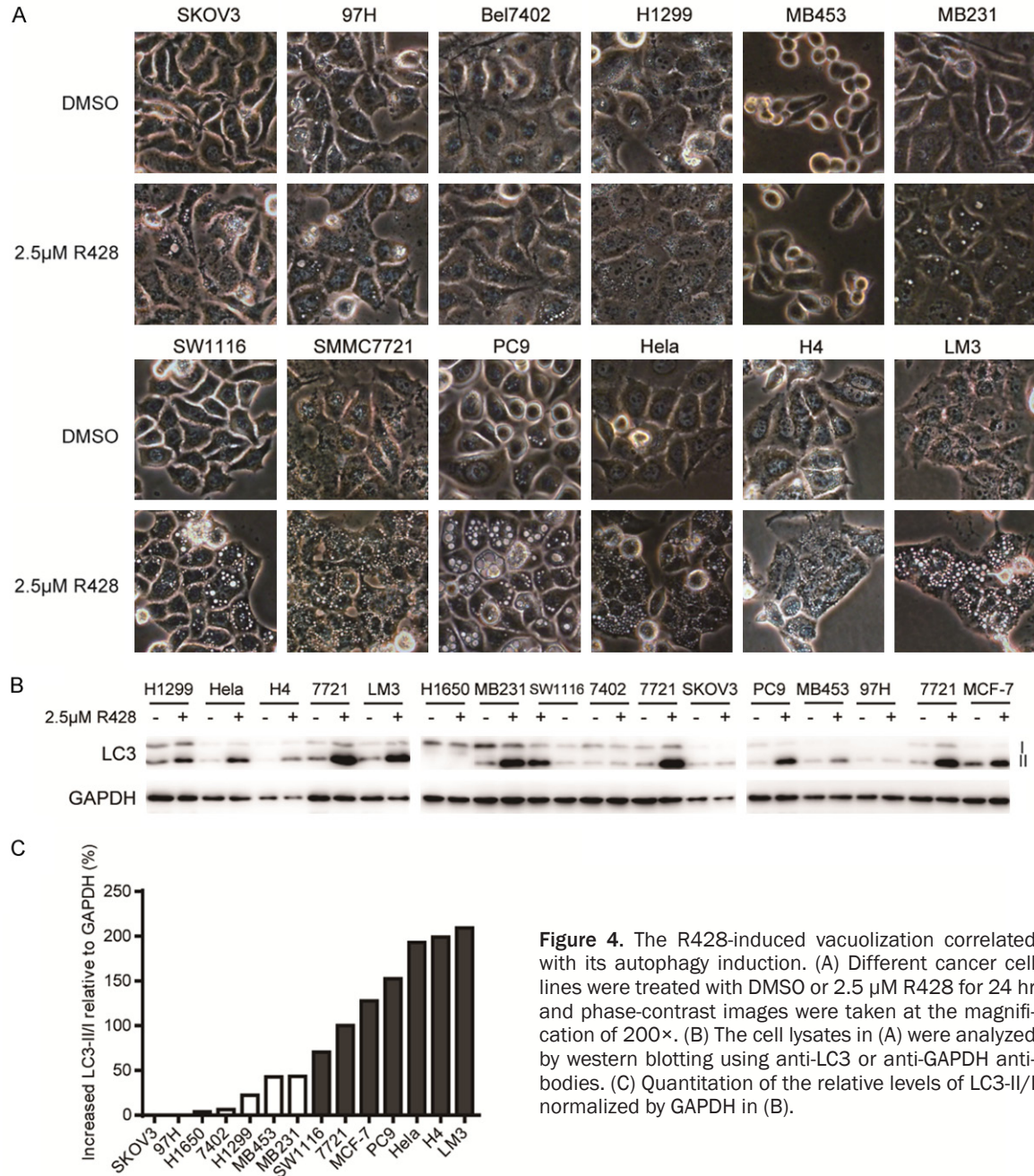


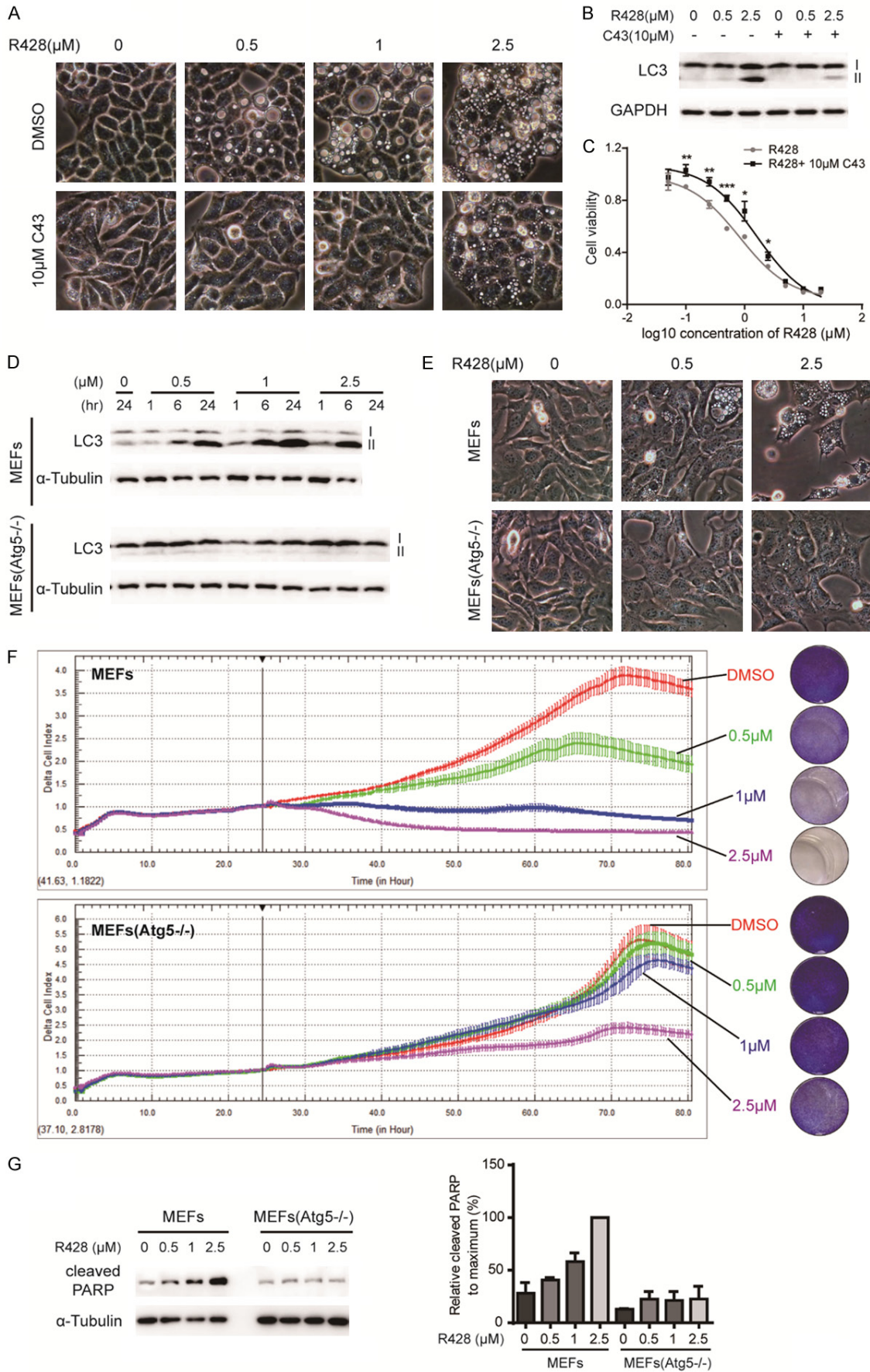
Figure 4. The R428-induced vacuolization correlated with its autophagy induction. (A) Different cancer cell lines were treated with DMSO or 2.5 µM R428 for 24 hr and phase-contrast images were taken at the magnification of 200×. (B) The cell lysates in (A) were analyzed by western blotting using anti-LC3 or anti-GAPDH antibodies. (C) Quantitation of the relative levels of LC3-II/I normalized by GAPDH in (B).

autophagy [34, 35]. R428 treatment increased the level of LC3-II, indicating the induction of autophagy initiation, but did not decrease the level of p62, suggesting a blockage of autophagic degradation (Figure 3C), in accordance with SB203580 (Figure S2C). As a control, the autophagy inducer rapamycin induced both LC3-II accumulation and p62 degradation (Figure 3C). A high fraction of the rapamycin-induced GFP-LC3 positive organelles were also stained by the lyso-tracker (Figure 3D), indicating the for-

mation of autolysosomes [36]. However, there was few double-positive autolysosomes in the R428-treated cells (Figures 3D and S2D), confirming that R428 inhibited the formation of normal autolysosomes and therefore blocked the autophagic degradation.

Thus, these results demonstrated that R428 interfered with lysosomal acidification, altered lysosomal function, and blocked autophagic degradation.

R428 induces cancer cell apoptosis by blocking lysosomal acidification



R428 induces cancer cell apoptosis by blocking lysosomal acidification

Figure 5. Inhibition of autophagic flux alleviated R428-induced vacuolization and growth inhibition as well as apoptosis. A. Bel7404 cells were incubated with R428 with or without 10 μ M C43 for 48 hr. Phase-contrast images were taken at the magnification of 200 \times . B. Bel7404 cells were incubated with R428 with or without 10 μ M C43 for 48 hr. The cell lysates were analyzed by western blot using anti-LC3. Anti-GAPDH was used as a control. C. Bel7404 cells were incubated with R428 with or without concomitant 10 μ M C43 for 72 hr. Cell viability was evaluated by MTT assay. *, $P < 0.05$; **, $P < 0.01$; ***, $P < 0.001$. Student's T test. Error bars, mean \pm SD. D. MEFs or MEFs (Atg5 $^{-/-}$) cells were treated with indicated concentration of R428 for indicated time. The cell lysates were analyzed by western blot using anti-LC3 and anti- α -tubulin. E. MEFs or MEFs (Atg5 $^{-/-}$) cells were treated with indicated concentration of R428 for 24 hr. Phase-contrast images were taken at the magnification of 200 \times . F. MEFs or MEFs (Atg5 $^{-/-}$) cells were treated with indicated concentration of R428 for indicated time. Cell viabilities were monitored by xCELLigence system in real time (left panel) or clone formation assay with crystal violet staining after 72hr-R428 treatment (right panel). Black lines in left panel marked the start point of drug administration. G. MEFs or MEFs (Atg5 $^{-/-}$) cells were treated with indicated concentration of R428 for 36 hr. The cell lysates were analyzed by western blot using anti-cleaved PARP and anti- α -tubulin. The histogram on the right calculated the relative levels of the cleaved PARP normalized by α -tubulin.

The R428-induced vacuolization correlated with its autophagy induction

As described above, the R428-induced lysosomal vacuolization caused autophagy initiation while blocked its progression. To clarify the relationship between vacuoles formation and autophagy, we compared the degree of autophagy initiation (increased LC3-II/I level) and vacuolization in different types of cancer cells and found a good correlation between the two (**Figure 4**). These results suggested that the R428-induced autophagy initiation might play an important role in vacuoles formation.

Inhibition of autophagy initiation alleviated the R428-induced vacuolization and growth inhibition

Above data revealed a correlation between autophagy initiation and vacuolization. To understand the causal relationship between the R428-induced autophagy initiation and vacuolization, we blocked the initiation of autophagy with spautin-1 (C43) and pyrvinium pamoate (PP), two autophagy inhibitors that affect early steps of autophagy [37, 38], and examined their effects on the R428-induced vacuoles formation. As shown in **Figures 5A** and **S3**, both inhibitors significantly reduced the numbers of the R428-induced vacuoles, as well as the LC3-II level (**Figures 5A**, **5B** and **S3**), demonstrating that inhibition of autophagy initiation alleviated the R428-induced vacuoles formation and that R428 acted after the formation of autophagosomes. C43 also alleviated the R428-induced cell death (**Figure 5C**), suggesting that the induction of autophagy contributed to the R428-induced cell death.

To further understand the role of autophagy in the R428-induced apoptosis, we examined the

effects of Atg5-knockout, which affects the stability of the LC3 system and blocks autophagy [39], on the R428-induced apoptosis using the Atg5-knockout MEF cells [17]. Consistent with the results of C43, Atg5-knockout significantly reduced the R428-induced vacuoles formation as well as apoptosis (**Figure 5D-G**).

Taken together, these data suggested that it was the combination of a blockage of autophagic degradation and an induction of autophagy by R428 that caused the continuous fusion of autolysosome to form large vacuoles, which sent a death signal to the cells to induce apoptosis.

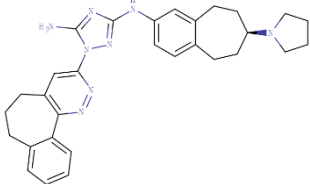
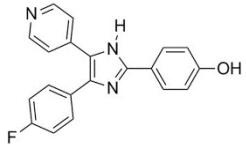
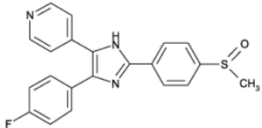
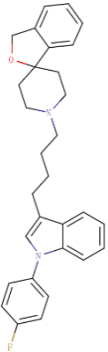
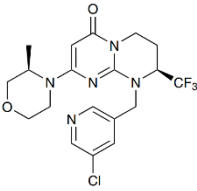
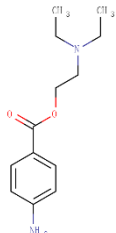
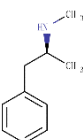
Discussion

R428 is an Axl inhibitor and a promising anti-cancer drug candidate, but its molecular mechanisms of inhibiting cancer cell growth, particularly the roles of inhibiting Axl, have not been well understood. In this study, we discovered a new activity and mechanism of R428 that induced apoptosis of cancer cells independent of Axl inhibition. We present evidences to suggest that lysosome was another target of R428. A protonation and accumulation of R428 in lysosomes altered lysosomal acidification, inhibited protein degradation, and blocked lysosome recycling, resulting in lysosomal deformation (vacuolization) and apoptotic cell death, all of which were independent of Axl inhibition.

Our data demonstrated that R428 was a potent but transient Axl inhibitor in cells. It inhibited the phosphorylation of Axl immediately after addition to the cells, but the phosphorylation of Axl bounced back shortly after the treatment and increased even higher 24 hours later (**Figures 1B** and **S1B**). The mechanisms of this change in phosphorylation were not clear. We

R428 induces cancer cell apoptosis by blocking lysosomal acidification

Table 1. Drugs reported to induce cytoplasmic vacuolation

Drug Name	Structure	Reference
R428		
SB202190		[19]
SB203580		[19]
Siramesine		[47]
SAR405		[48]
Procaine		[33, 49]
Methamphetamine		[50]

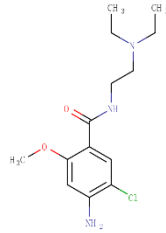
analyzed the mRNA expression of the Axl ligand Gas6 after R428 treatment but found no change in the Gas6 expression (Figure S1A). We however found that the expression of Axl protein was increased 24 hours after R428 treatment (Figures 1B and 2F). It is possible that the increased Axl protein stimulated transphosphorylation of itself. On the contrary, another Axl inhibitor LDC1267 suppressed the phosphorylation of Axl effectively for more than 24 hours (Figure 1B), suggesting that the R428-induced later increase in Axl phosphorylation was a specific response of the cells to other targets of R428, possibly lysosomal dysfunction, induction of autophagy, or apoptosis.

R428 is an amine-containing lipophilic compound. Several compounds with similar structural properties of R428 have also been reported to induce cytoplasmic vacuolization (Table 1). All of them are rich in tertiary amine or secondary amine groups thus presenting alkalescence (Table 1). These weakly basic molecules are lysosomotropic and accumulate extensively in the acidic organelles through ion trapping [40, 41]. In addition to R428, we tested another weak basic lipophilic drug SB203580, a specific inhibitor of p38 MAPK, and found that it induced vacuolization in a similar way as that of R428 (Figure 3B). It is therefore possible that R428 was also trapped in the lysosomes so that it could no longer interact with Axl to maintain its continuous inhibition, which is in line with the observation that the Axl phosphorylation was only transiently inhibited by R428 (Figure 1B). In this regard, the lysosomotropic property of R428 may weaken it as an inhibitor of Axl and its use as a clinic drug against cancer metastasis.

Axl has also been reported to play a role in regulating autophagy but its roles were different in different circumstances. Activation of Axl stimulated autophagy and prevented proin-

R428 induces cancer cell apoptosis by blocking lysosomal acidification

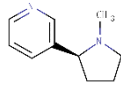
Metoclopramide



[33]

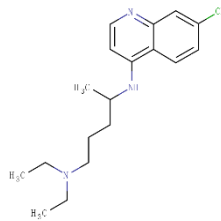
autophagy initiation was independent of Axl (**Figure 2F**).

Nicotine



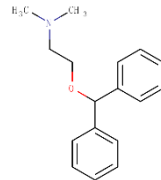
[33]

Chloroquine



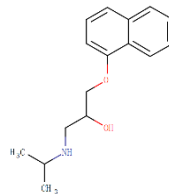
[33]

Diphenhydramine



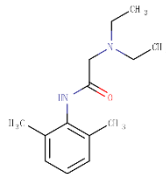
[33]

Propranolol



[33]

Lidocaine



[49]

flammatory cytokine secretion in macrophages to reduce liver injury [42], whereas downregulation of Axl expression was reported to induce autophagy and apoptosis in certain cancer cells [43, 44]. R428 induced autophagy initiation as well as a later activation of Axl (**Figures 1B** and **3C**). Because the R428-induced Axl activation occurred much later (more than 6 hours) than the induction of autophagy initiation (less than 1 hour), it is unlikely that the R428-induced autophagy initiation was a consequence of Axl activation. Our Axl knock-down experiments confirmed that the R428-induced

The direct effect of R428 on cells was the induction of large single membrane-bounded vacuoles. The lysosomal origin of the vacuoles was supported by several lines of evidences. First, the lysosomal-associated protein-GFP fusion protein, Lamp1-GFP was found to be present in both lysosomes and the vacuoles, suggesting that the two shared the same origin. Second, the TEM analyses identified similar dense materials inside the vacuoles as those in lysosomes. Third, the differential staining of the vacuoles with the three chromogenic acidic tracers, NR, AO, or lyso-tracker, confirmed the lysosome-like acidic nature of the vacuoles (**Figures 2C, 3A** and **S2A**). Furthermore, neutralization of the lysosomal pH with two lysosomal lumen alkalizers, Baf A1 or CQ, completely abolished the R428-induced vacuoles formation (**Figure 3B**), further supporting that the lysosome was the target of R428. It is likely that the neutralization of lysosomes by Baf A1 or CQ changed their pH and prevented the protonation and accumulation of R428 in the lysosomes and consequently the concomitant lysosomal dilation.

We also observed increased number of autophagosomes and lysosomes (**Figures 2D** and **S2B**), indicating an induction of autophagy. Indeed, the transcriptions of the autophagy-related genes were stimulated by R428 (**Figure 2G**), suggesting that a feedback signal was induced by the disruption of autophagic protein degradation in the lysosomes. Consistent with our data, other lysosomal inhibitors, such as Baf A1 and ConA, were reported to trigger autophagy initiation via inhibiting the negative regulator of autophagy mTORC1 (mTOR complex 1) [46]. Inhibition of autophagy with autophagy inhibitors, C43, PP, CQ, or Baf A1, blocked the R428-induced vacuoles formation as well as apoptosis, supporting that autophagy is required for the vacuoles formation and apoptosis.

R428 induces cancer cell apoptosis by blocking lysosomal acidification

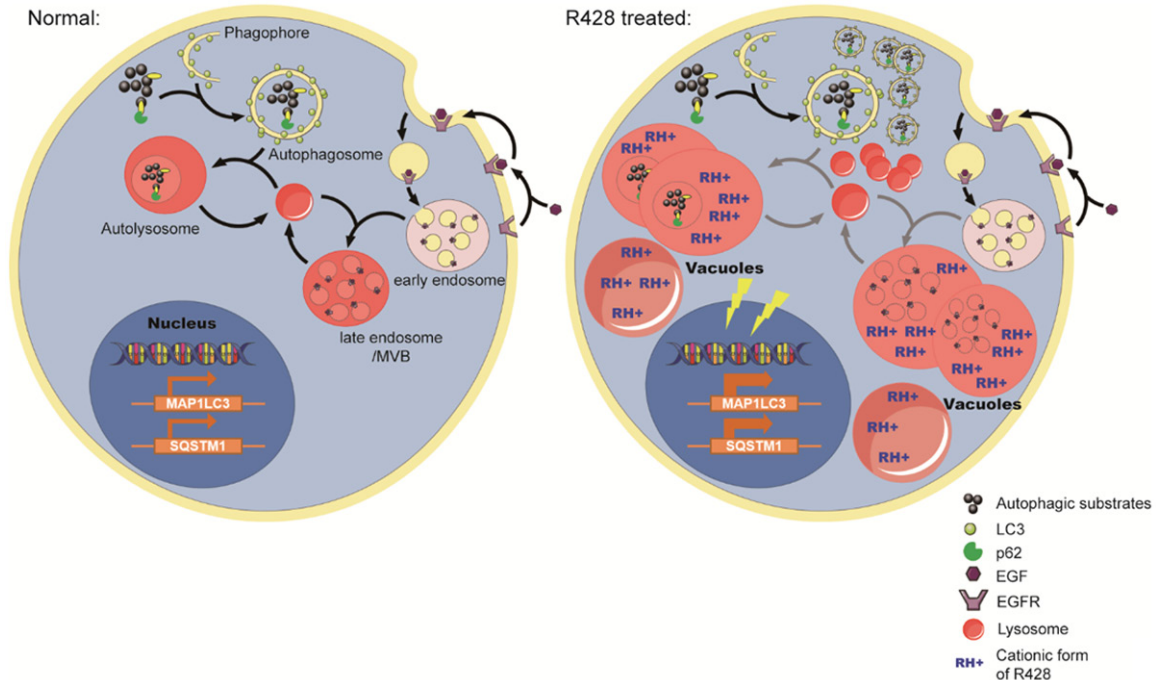


Figure 6. A schematic model of R428 action. Left: The normal lysosomal degradation involves packaging of autophagic substrates (eg. dysfunctional organelles and proteins) and membrane receptors (eg. EGFR, Figure S4) into autophagosomes and early endosomes and then a fusion with lysosomes to form autolysosomes and late endosomes (multivesicular bodies, MVBs) to degrade the contents by lysosomal hydrolases, followed by recycling back to lysosomes via lysosomal acidification and maturation. Right: Upon R428 treatment, the unprotonated R428s (R) diffuse into the acidic organelles becoming protonated (RH+) and are trapped there, which increases osmotic pressure to enlarge the lysosomes and the other acidic organelles, including endosomes and autolysosomes. They are rapidly alkalified by R428 and subsequently deprived of protein degradation ability because of high pH. Alteration of lysosome function causes lysosome deformation and vacuoles formation, which in turn sends signals to induce autophagy leading to more vacuoles formation. The excessive vacuoles eventually induce apoptosis of the cells.

It is not entirely clear what the molecular events linking the R428-induced vacuoles formation and apoptosis are. Our data suggested that the blockage of lysosome function might play a key role. Studies on the two lysosomal lumen alkalinizers, Baf A1 or CQ-induced apoptosis have identified mitochondria as the mediator of the caspase activation and apoptosis [32, 45]. Thus, it is plausible that R428 may act in a similar fashion since all of them alkalify acidic organelles and disable lysosomes.

In summary, our data suggests a model to illustrate the mechanisms of R428 in inducing vacuoles formation and apoptosis (Figure 6). These data uncovered new targets and activities of R428, which would help to better understand and further develop R428 into a more effective and less toxic anti-cancer agent. It also added new knowledge on the understanding of the regulation of autophagy and apoptosis.

Acknowledgements

This work was supported by the National Natural Science Foundation of China (No. 81673465, 81373447 to Qiang Yu), the China Ministry of Science and Technology Key New Drug Creation and Manufacturing Program (No. 2014ZX09102001-002 to Qiang Yu), and the China National Key Basic Research Program (No. 2013CB910904 to Qiang Yu). We are grateful to Prof. Junying Yuan for providing chemicals and cell lines and Prof. Jing Yi for technical assistance of TEM analyses.

Disclosure of conflict of interest

None.

Address correspondence to: Dr. Qiang Yu, Shanghai Institute of Materia Medica, Chinese Academy of Sciences, 555 Zuchongzhi Road, Room 2-225, Shanghai 201203, China. Tel: 86 2150801790; Fax: 86 2150800306; E-mail: qyu@sibs.ac.cn

References

- [1] Axelrod H, Pienta KJ. Axl as a mediator of cellular growth and survival. *Oncotarget* 2014; 5: 8818-8852.
- [2] Holland SJ, Pan A, Franci C, Hu Y, Chang B, Li W, Duan M, Torneros A, Yu J, Heckrodt TJ, Zhang J, Ding P, Apatira A, Chua J, Brandt R, Pine P, Goff D, Singh R, Payan DG and Hitoshi Y. R428, a selective small molecule inhibitor of Axl kinase, blocks tumor spread and prolongs survival in models of metastatic breast cancer. *Cancer Res* 2010; 70: 1544-1554.
- [3] Wu X, Liu X, Koul S, Lee CY, Zhang Z and Halmos B. AXL kinase as a novel target for cancer therapy. *Oncotarget* 2014; 5: 9546-9563.
- [4] Brown M, Black JR, Sharma R, Stebbing J and Pinato DJ. Gene of the month: Axl. *J Clin Pathol* 2016; 69: 391-397.
- [5] Ahsan A. Mechanisms of resistance to EGFR tyrosine kinase inhibitors and therapeutic approaches: an update. *Adv Exp Med Biol* 2016; 893: 137-153.
- [6] Asish K. Ghosh CS, Justin Boysen, Traci Sassoon, Tait D. Shanafelt, Debabrata Mukhopadhyay, and Kay NE. The novel receptor tyrosine kinase Axl is constitutively active in B-cell chronic lymphocytic leukemia and acts as a docking site of nonreceptor kinases: implications for therapy. *Blood* 2011; 117: 1928-1937.
- [7] Smolock EM and Korshunov VA. Pharmacological inhibition of Axl affects smooth muscle cell functions under oxidative stress. *Vascul Pharmacol* 2010; 53: 185-192.
- [8] Mathew R, Karantza-Wadsworth V, White E. Role of autophagy in cancer. *Nat Rev Cancer* 2007; 7: 961-7.
- [9] Shen J, Zheng H, Ruan J, Fang W, Li A, Tian G, Niu X, Luo S and Zhao P. Autophagy inhibition induces enhanced proapoptotic effects of ZD6474 in glioblastoma. *Br J Cancer* 2013; 109: 164-171.
- [10] Mizushima N. Autophagy: process and function. *Genes Dev* 2007; 21: 2861-2873.
- [11] Chen Y and Yu L. Recent progress in autophagic lysosome reformation. *Traffic* 2017; 18: 358-361.
- [12] Shen HM and Mizushima N. At the end of the autophagic road: an emerging understanding of lysosomal functions in autophagy. *Trends Biochem Sci* 2014; 39: 61-71.
- [13] Marino G, Niso-Santano M, Baehrecke EH and Kroemer G. Self-consumption: the interplay of autophagy and apoptosis. *Nat Rev Mol Cell Biol* 2014; 15: 81-94.
- [14] Mukhopadhyay S, Panda PK, Sinha N, Das DN and Bhutia SK. Autophagy and apoptosis: where do they meet? *Apoptosis* 2014; 19: 555-566.
- [15] Sherer NM LM, Jimenez-Soto LF, Ingmundson A, Horner SM, Cicchetti G, Allen PG, Pypaert M, Cunningham JM, Mothes W. Visualization of retroviral replication in living cells reveals budding into multivesicular bodies. *Traffic* 2003; 4: 785-801.
- [16] Zhang L, Yu J, Pan H, Hu P, Hao Y, Cai W, Zhu H, Yu AD, Xie X, Ma D and Yuan J. Small molecule regulators of autophagy identified by an image-based high-throughput screen. *Proc Natl Acad Sci U S A* 2007; 104: 19023-19028.
- [17] Hosokawa N, Hara Y and Mizushima N. Generation of cell lines with tetracycline-regulated autophagy and a role for autophagy in controlling cell size. *FEBS Lett* 2006; 580: 2623-2629.
- [18] Sun X, Song Q, He L, Yan L, Liu J, Zhang Q and Yu Q. Receptor tyrosine kinase phosphorylation pattern-based multidrug combination is an effective approach for personalized cancer treatment. *Mol Cancer Ther* 2016; 15: 2508-2520.
- [19] Manoj B. Menon AK, Matthias Gaestel. SB202-190-induced cell type-specific vacuole formation and defective autophagy do not depend on p38 MAPKinase inhibition. *PLoS One* 2011; 6: 1-13.
- [20] Guo H, Kuang S, Song QL, Liu M, Sun XX and Yu Q. Cucurbitacin I inhibits STAT3, but enhances STAT1 signaling in human cancer cells in vitro through disrupting actin filaments. *Acta Pharmacol Sin* 2018; 39: 425-437.
- [21] Sun X, Ai M, Wang Y, Shen S, Gu Y, Jin Y, Zhou Z, Long Y and Yu Q. Selective induction of tumor cell apoptosis by a novel P450-mediated reactive oxygen species (ROS) inducer methyl 3-(4-nitrophenyl) propionate. *J Biol Chem* 2013; 288: 8826-8837.
- [22] Zhang Q, Wu S, Zhu J, Chai D and Gan H. Down-regulation of ASIC1 suppressed gastric cancer via inhibiting autophagy. *Gene* 2017; 608: 79-85.
- [23] Mo R, Tony Zhu Y, Zhang Z, Rao SM and Zhu YJ. GAS6 is an estrogen-inducible gene in mammary epithelial cells. *Biochem Biophys Res Commun* 2007; 353: 189-194.
- [24] Paolino M, Choidas A, Wallner S, Pranjić B, Uribealago I, Loeser S, Jamieson AM, Langdon WY, Ikeda F, Fededa JP, Cronin SJ, Nitsch R, Schultz-Fademrecht C, Eickhoff J, Menninger S, Unger A, Torika R, Gruber T, Hinterleitner R, Baier G, Wolf D, Ullrich A, Klebl BM and Penninger JM. The E3 ligase Cbl-b and TAM receptors regulate cancer metastasis via natural killer cells. *Nature* 2014; 507: 508-512.
- [25] Wu J, Hu G, Dong Y, Ma R, Yu Z, Jiang S, Han Y, Yu K and Zhang S. Matrine induces Akt/mTOR signalling inhibition-mediated autophagy and apoptosis in acute myeloid leukaemia cells. *J Cell Mol Med* 2017; 21: 1171-1181.

R428 induces cancer cell apoptosis by blocking lysosomal acidification

- [26] Luzio JP, Pryor PR and Bright NA. Lysosomes: fusion and function. *Nat Rev Mol Cell Biol* 2007; 8: 622-632.
- [27] Pierzynska-Mach A, Janowski PA and Dobrucki JW. Evaluation of acridine orange, LysoTracker Red, and quinacrine as fluorescent probes for long-term tracking of acidic vesicles. *Cytometry A* 2014; 85: 729-737.
- [28] Rubinsztein DC, Cuervo AM, Ravikumar B, Sarkar S, Korolchuk VI, Kaushik S and Klionsky DJ. In search of an "autophagometer". *Autophagy* 2014; 5: 585-589.
- [29] Hayato Takeuchi YK, Keishi Fujiwara, Takao Kanzawa, Hiroshi Aoki, Gordon B. Mills, and Seiji Kondo Synergistic augmentation of rapamycin-induced autophagy in malignant glioma cells by phosphatidylinositol 3-kinase/protein kinase B inhibitors. *Cancer Res* 2005; 65: 3336-3346.
- [30] Liu J, Xia H, Kim M, Xu L, Li Y, Zhang L, Cai Y, Norberg HV, Zhang T, Furuya T, Jin M, Zhu Z, Wang H, Yu J, Li Y, Hao Y, Choi A, Ke H, Ma D and Yuan J. Beclin1 controls the levels of p53 by regulating the deubiquitination activity of USP10 and USP13. *Cell* 2011; 147: 223-234.
- [31] Anes E, Kuhnle MP, Bos E, Moniz-Pereira J, Habermann A and Griffiths G. Selected lipids activate phagosome actin assembly and maturation resulting in killing of pathogenic mycobacteria. *Nat Cell Biol* 2003; 5: 793-802.
- [32] Harhaji-Trajkovic L, Arskin K, Kravic-Stevovic T, Petricevic S, Tovilovic G, Pantovic A, Zogovic N, Ristic B, Janjetovic K, Bumbasirevic V and Trajkovic V. Chloroquine-mediated lysosomal dysfunction enhances the anticancer effect of nutrient deprivation. *Pharm Res* 2012; 29: 2249-2263.
- [33] Morissette G, Moreau E, C-Gaudreault R, Marceau F. Massive cell vacuolization induced by organic amines such as procainamide. *J Pharmacol Exp Ther* 2004; 310: 395-406.
- [34] Pankiv S, Clausen TH, Lamark T, Brech A, Bruun JA, Outzen H, Overvatn A, Bjorkoy G and Johansen T. p62/SQSTM1 binds directly to Atg8/LC3 to facilitate degradation of ubiquitinated protein aggregates by autophagy. *J Biol Chem* 2007; 282: 24131-24145.
- [35] Shimizu S, Takehara T, Hikita H, Kodama T, Tsunematsu H, Miyagi T, Hosui A, Ishida H, Tsumi T, Kanto T, Hiramatsu N, Fujita N, Yoshimori T and Hayashi N. Inhibition of autophagy potentiates the antitumor effect of the multikinase inhibitor sorafenib in hepatocellular carcinoma. *Int J Cancer* 2012; 131: 548-557.
- [36] Park YE, Hayashi YK, Bonne G, Arimura T, Noguchi S, Nonaka I and Nishino I. Autophagic degradation of nuclear components in mammalian cells. *Autophagy* 2014; 5: 795-804.
- [37] Liu J, Xia H, Kim M, Xu L, Li Y, Zhang L, Cai Y, Norberg HV, Zhang T, Furuya T, Jin M, Zhu Z, Wang H, Yu J, Li Y, Hao Y, Choi A, Ke H, Ma D and Yuan J. Beclin1 controls the levels of p53 by regulating the deubiquitination activity of USP10 and USP13. *Cell* 2011; 147: 223-234.
- [38] Deng L, Lei Y, Liu R, Li J, Yuan K, Li Y, Chen Y, Liu Y, Lu Y, Edwards CK 3rd, Huang C and Wei Y. Pyruvate targets autophagy addiction to promote cancer cell death. *Cell Death Dis* 2013; 4: e614.
- [39] Walczak M, Martens S. Dissecting the role of the Atg12-Atg5-Atg16 complex during autophagosome formation. *Autophagy* 2013; 9: 424-425.
- [40] Funakoshi T, Aki T, Unuma K and Uemura K. Lysosome vacuolation disrupts the completion of autophagy during norephedrine exposure in SH-SY5Y human neuroblastoma cells. *Brain Res* 2013; 1490: 9-22.
- [41] Ndolo RA, Luan Y, Duan S, Forrest ML, Krise JP. Lysosomotropic properties of weakly basic anticancer agents promote cancer cell selectivity in vitro. *PLoS One* 2012; 7: e49366.
- [42] Su Z, Yang Z, Xu Y, Chen Y and Yu Q. Apoptosis, autophagy, necroptosis, and cancer metastasis. *Mol Cancer* 2015; 14: 48.
- [43] Keating AK, Kim GK, Jones AE, Donson AM, Ware K, Mulcahy JM, Salzberg DB, Foreman NK, Liang X, Thorburn A and Graham DK. Inhibition of Mer and Axl receptor tyrosine kinases in astrocytoma cells leads to increased apoptosis and improved chemosensitivity. *Mol Cancer Ther* 2010; 9: 1298-1307.
- [44] Gaur S, Wen Y, Song JH, Parikh NU, Mangala LS, Blessing AM, Ivan C, Wu SY, Varkaris A, Shi Y, Lopez-Berestein G, Frigo DE, Sood AK, Gallik GE. Chitosan nanoparticle-mediated delivery of miRNA-34a decreases prostate tumor growth in the bone and its expression induces non-canonical autophagy. *Oncotarget* 2015; 6: 29161-29177.
- [45] Shacka JJ, Klocke BJ, Shibata M, Uchiyama Y, Datta G, Schmidt RE and Roth KA. Bafilomycin A1 inhibits chloroquine-induced death of cerebellar granule neurons. *Mol Pharmacol* 2006; 69: 1125-1136.
- [46] Manoj B. Menon, Alexey Kotlyarov and Gaestel M. SB202190-induced cell type-specific vacuole formation and defective autophagy do not depend on p38 MAPKinase inhibition. *PLoS One* 2011; 6: 1-13.
- [47] Ostefeld MS, Høyer-Hansen M, Bastholm L, Fehrenbacher N, Olsen OD, Groth-Pedersen L, Puustinen P, Kirkegaard-Sørensen T, Nylandsted J, Farkas T and Jäättelä M. Anti-cancer agent siramesine is a lysosomotropic detergent that induces cytoprotective autophagosome accumulation. *Autophagy* 2014; 4: 487-499.
- [48] Ronan B, Flamand O, Vescovi L, Dureuil C, Durand L, Fassy F, Bachelot MF, Lambertson A,

R428 induces cancer cell apoptosis by blocking lysosomal acidification

- Mathieu M, Bertrand T, Marquette JP, El-Ahmad Y, Filoche-Romme B, Schio L, Garcia-Echeverria C, Goulaouic H and Pasquier B. A highly potent and selective Vps34 inhibitor alters vesicle trafficking and autophagy. *Nat Chem Biol* 2014; 10: 1013-1019.
- [49] Bawolak MT, Morissette G and Marceau F. Vacuolar ATPase-mediated sequestration of local anesthetics in swollen macroautophagosomes. *Can J Anaesth* 2010; 57: 230-239.
- [50] Nara A, Aki T, Funakoshi T and Uemura K. Methamphetamine induces macropinocytosis in differentiated SH-SY5Y human neuroblastoma cells. *Brain Res* 2010; 1352: 1-10.

R428 induces cancer cell apoptosis by blocking lysosomal acidification

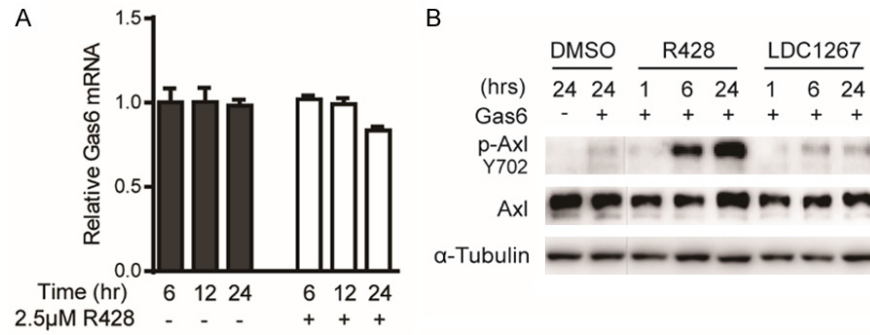


Figure S1. Effects of R428 on Gas6 mRNA expression and Gas6-stimulated Axl activation. A. RT-qPCR analysis of Gas6 mRNA expression in H1299 cells which were cultured with or without 2.5 μ M R428 for indicated time periods. Error bars, mean \pm SD. B. HeLa cells were cultured with DMSO, 2.5 μ M R428, or 0.5 μ M LDC1267 for indicated time periods and then stimulated with 200 ng/ml Gas6 for 15 min. Total cell lysates were processed for western blotting analyses using antibodies as indicated.

R428 induces cancer cell apoptosis by blocking lysosomal acidification

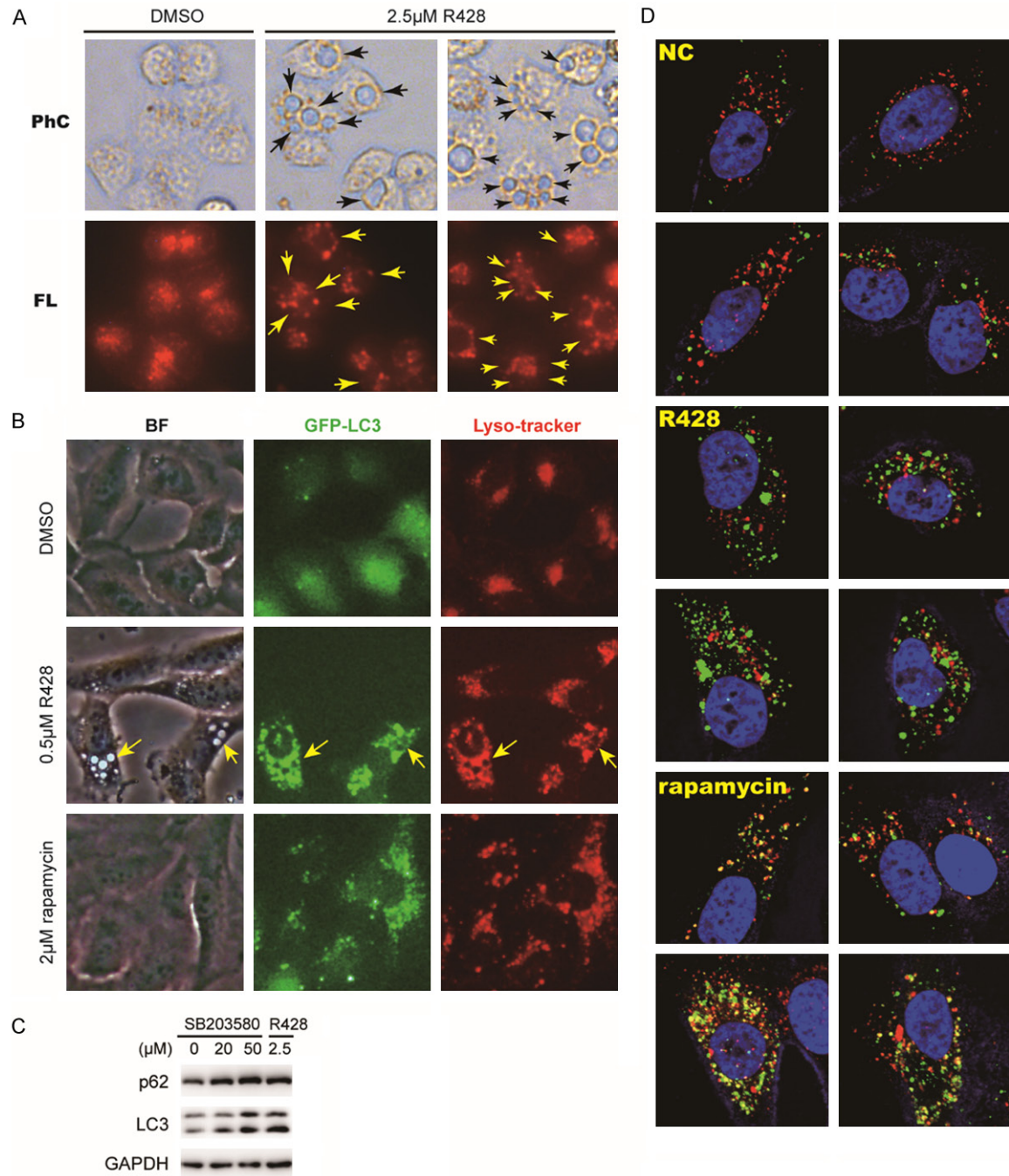


Figure S2. R428 altered lysosomal acidification and inhibited autolysosomes formation. **A.** Bel7404 cells were cultured with DMSO or 2.5 μ M R428 for 24 hr and stained with lysosome-tracker red. Arrows point to the enlarged vacuoles. **B.** H4-GFP-LC3 cells were treated with DMSO, 0.5 μ M R428, or 2 μ M rapamycin for 24 hr, and then stained with lysosome-tracker red. Formation of GFP-LC3 puncta and lysosomes were visualized by fluorescence microscopy. Yellow arrows point to the enlarged vacuoles. Magnification: \times 200. **C.** H4-GFP-LC3 cells were lysed after treatment with SB203580 or R428 for 24 hr. The cell lysates were analyzed by western blotting using antibodies as indicated. Anti-GAPDH antibody was used as a loading control. **D.** H4-GFP-LC3 cells were cultured with DMSO, 2.5 μ M R428 or 2 μ M rapamycin for 24 hr, then stained with lysosome-tracker. Fixed samples were visualized by confocal microscopy. 2 μ g/ml Hoechst dye was used to stain nucleus.

R428 induces cancer cell apoptosis by blocking lysosomal acidification

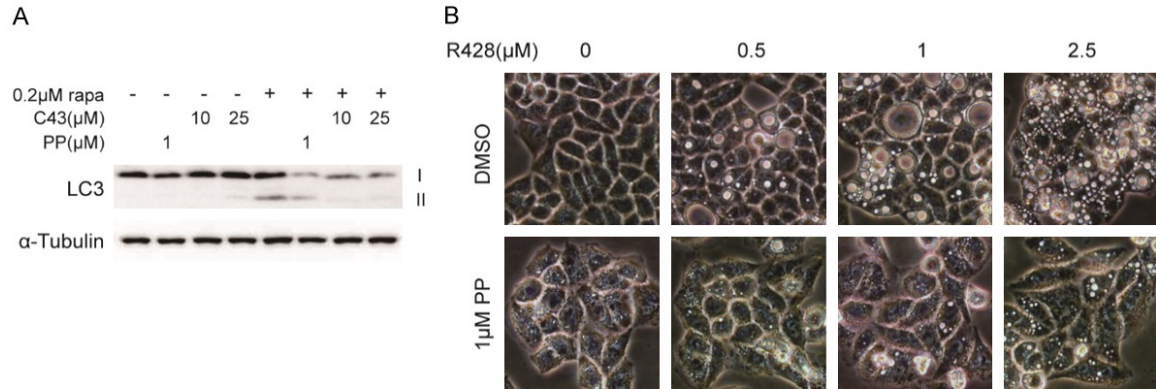


Figure S3. The R428-induced vacuoles formation were alleviated by autophagy inhibitors. A. H4-GFP-LC3 cells were cultured with C43 or PP with or without rapamycin for 6 hr. The whole cell lysates were analyzed by western blotting using anti-LC3 and anti- α -tubulin. B. Bel7404 cells were cultured with R428 with or without PP for 48 hr. Phase-contrast images were taken at the magnification of 200 \times .

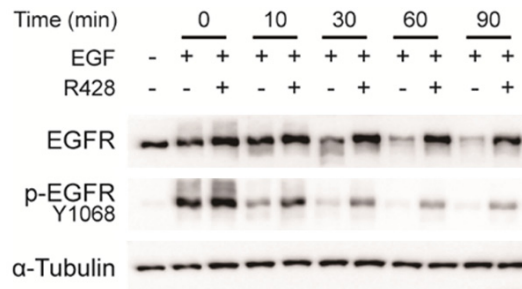


Figure S4. R428 inhibited endocytosis of EGFR. H4-GFP-LC3 cells were cultured under serum starvation condition overnight to recruit all the EGF receptors to plasma membrane. 100 ng/ml EGF was added for 10 min at 37 $^{\circ}$ C. The cells were then cultured in DMEM with or without 2.5 μ M R428 for indicated time periods and the whole cell lysates were analyzed by western blotting using anti-EGFR, anti-pEGFR, or anti- α -tubulin antibody.